HVAC&R Research
Publication details, including instructions for authors and subscription information:
http://www.tandfonline.com/loi/uhvc20

Simplified thermal modeling of indirect evaporative heat exchangers

Zhijun Liu [a], William Allen [a] & Mark Modera [a]
[a] Western Cooling Efficiency Center, University of California, Davis, 215 Sage Street, Suite 100, Davis, CA, 95618, USA
Accepted author version posted online: 15 Jan 2013.Published online: 28 Apr 2013.

To cite this article: Zhijun Liu , William Allen & Mark Modera (2013) Simplified thermal modeling of indirect evaporative heat exchangers, HVAC&R Research, 19:3, 257-267

To link to this article: http://dx.doi.org/10.1080/10789669.2013.763653

HVAC&R Research (2013) **19**, 257–267

ISSN: 1078-9669 print / 1938-5587 online
DOI: 10.1080/10789669.2013.763653

Taylor & Francis
Taylor & Francis Group

Simplified thermal modeling of indirect evaporative heat exchangers

ZHIJUN LIU*, WILLIAM ALLEN, and MARK MODERA

Western Cooling Efficiency Center, University of California, Davis, 215 Sage Street, Suite 100, Davis CA, 95618, USA

A simplified model using a modified effectiveness–Number of Transfer Units (NTU) method for thermal performance simulation of indirect evaporative heat exchangers is presented and then validated utilizing experimental data from the literature. The objective of this model is to facilitate efficient computer simulation of indirect evaporative cooling or hybrid indirect evaporative cooling/direct expansion vapor compression systems, both of which include an indirect evaporative heat exchanger as a core component. Through some approximations, the governing differential equations that describe indirect evaporative heat exchanger heat/mass transfer behavior are modified to produce a methodology that is analogous to the effectiveness–NTU method for sensible-only heat exchangers. The simplified set of equations can then be solved within short computation times and with numerical stability. An examination of the Lewis factor impact on evaporation processes using this model indicates that the approximation of unity for the Lewis factor may not be valid when the inlet air to the wet side is cold and dry.

Introduction

Indirect evaporative cooling (IEC) is a water-based cooling technology that is attractive for space cooling in dry and hot climates due to its lower energy consumption (compared to vapor compression air conditioners) and lack of humidification (compared to direct evaporative cooling) (Maheshwari et al. 2001). Among the components incorporated into advanced IEC or hybrid IEC/direct expansion (DX) systems (Elberling 2006), the indirect evaporative heat exchanger (IEHX) is the most critical, as it is the core technology or "heart" of the system.

A typical IEHX consists of a series of thin parallel plates assembled to form a multi-layer sandwich of alternating dry and wet channels. The primary (supply) air (to room) is cooled in the dry channel (without the addition of moisture) by evaporating water into the secondary (exhaust) air stream in the wet channel and allowing the cool air in the wet channel to absorb heat from the warmer dry channel.

There are many possible configurations for IEHX designs, and their performance is heavily dependent on the operating conditions and climate in which they are applied (Erens and Dreyer 1993). To characterize the thermal behaviors of these coolers and to support their implementation by HVAC designers, a practical, accurate IEHX model is needed. To be most useful, the model should be incorporated into building simulation packages, (e.g., EnergyPlus). To simulate the performance of an IEC or hybrid IEC/DX system in different operating conditions using building simulation packages, hundreds and even thousands of simulations may be required. In this case, reduced computation time is crucial. In addition, detailed IEHX characterization data (i.e., IEHX surface geometries and heat transfer coefficients) are often scarce, and HVAC designers may only rely on performance data from the manufacturers' product catalogs.

Typically, there are two approaches for IEHX analysis, namely the numerical (finite difference/element) approach and the analytical approach. The numerical approach may satisfy the requirements of high accuracy, but it requires detailed IEHX characterization data as inputs, which are often not available for HVAC designers. It also needs some sophisticated numerical methods for solutions (Hsu et al. 1989),which may result in long computational times. The analytical approach usually treats the whole IEHX as a single element, and after making necessary simplifying assumptions, the controlling differential equations can then be integrated analytically, resulting in a fairly simple-to-use model.

This article attempts to address the above concerns via a simplified IEHX model for engineering practice. The model should fill the requirements of HVAC designers, including

- simplicity of data inputs,
- ability to model different operating conditions and climates,
- short computational time, and
- reasonable accuracy.

Methodology overview

Heat transfer in the dry channel of an IEHX is similar to that in a sensible heat exchanger, while heat and mass transfer in the wet channel is analogous to that in an

Received August 15, 2012; accepted December 5, 2012
Zhijun Liu, Student Member ASHRAE, is PhD student. **William Allen, PhD**, is Senior Engineer. **Mark Modera, PhD, PE**, Fellow ASHRAE, is Professor.
*Corresponding author e-mail: zjliu@ucdavis.edu

indirect-contact cooling tower, both of which have been studied extensively (Kloppers and Kroger 2005a; Kakac et al. 1987). For the thermal analysis of sensible heat exchangers, the classic effectiveness–Number of Transfer Units (NTU) method is widely used (Kays 1984). To predict the thermal performance of indirect-contact cooling towers, several simplified models have been proposed in place of the detailed model of Poppe and Rögener (1984). Those simplified models are analgous to the effectiveness-NTU method for sensible heat exchangers (Braun et al. 1989; ElDessouky et al. 1997; Stabat and Marchio 2004). The same methodology was also employed for liquid desiccant applications (Gandhidasan 2004) that involve simultaneous heat and mass transfer in channels. Most of the simplified models are based on Merkel's (1925) theory, which assumes a unity Lewis factor and neglects the water losses due to evaporation. Additional assumptions may also include the water film temperature being constant along the whole cooler and the enthalpy being a linear function of only the wet-bulb temperature.

A similar methodology can be adopted for thermal modeling of IEHXs, given that the heat and mass transfer process in an IEHX is essentially similar to that in an indirect-contact cooling tower. For instance, by assuming constant water film temperature throughout the wet channel, (Erens and Dreyer 1993) claimed the Merkel model can be integrated to find the outlet air temperatures of an IEHX. That model greatly reduces the simulation time but is less accurate for increased cooler capacity due to the assumption of constant water temperature. Recently, Hasan (2012) derived an effectiveness-NTU method for indirect evaporative coolers that uses the enthaply difference between the primary and secondary air streams as the driving force for heat transfer. The model introduces a coefficient a to represent the slope of the saturation line but does not discuss how to find its value, nor its impact to the model accuracy. Hasan's model was verified only in one operating condition without discussing its validation at different operating conditions.

In this article, a simplified model using a modified effectiveness-NTU method for IEHXs is presented and then validated utilizing experimental data from the literature in a wide range of operating conditions. The model highlights several improvements over the existing simplified models in the literature, including the detailed procedure for UA value calculation for laminar and turbulent IEHX channel flows.

Model formulation

The model is based on a steady-state heat-and-mass transfer balance. The main assumptions are

- steady, incompressible fluid flows that are thermally isolated from the surroundings;
- evenly distributed thin water film on the wet-channel surfaces;
- Lewis factor equal to one;
- heat/mass transfer normal to the direction of fluid flows only; and
- no condensation in the primary air channel.

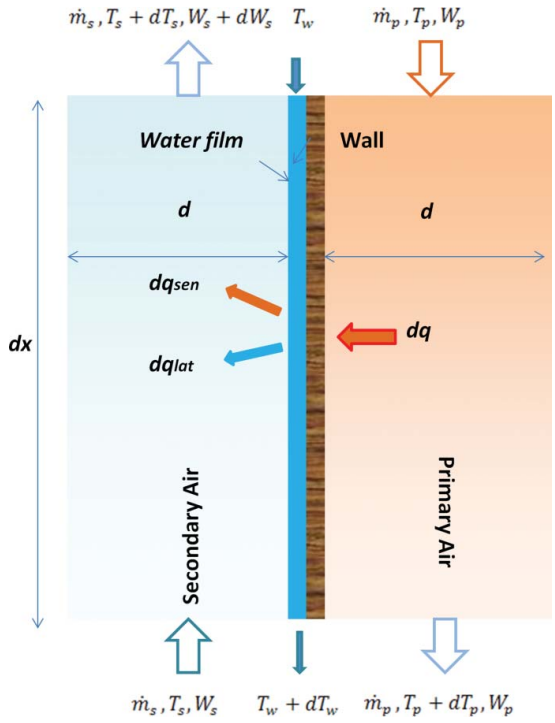

Fig. 1. Sketch of modeling element for a counter-flow IEHX (color figure available online).

Figure 1 illustrates the modeling element. Due to symmetry, only half of the dry and wet-channel gaps are considered.

As shown in Figure 1, heat transfer from the primary air stream (dry side) to the water film on the wet side of the heat exchanger is driven by the temperature difference between those two streams. In other words,

$$dq = U_{p-w} dA_p (T_p - T_w), \tag{1}$$

where U_{p-w} is the overall heat transfer coefficient between the primary air stream and the water film:

$$U_{p-w} = \frac{1}{h_p} + \frac{\delta}{k} + \frac{\delta_w}{k_w}. \tag{2}$$

For the primary air stream, conservation of energy implies that dq can also be expressed as

$$dq = \dot{m}_p c_{pa} dT_p. \tag{3}$$

Heat transfer from the water film to the secondary air is driven by the enthalpy difference between the secondary air stream and the saturated water–air interface vapor layer (Bourdouxhe et al. 1994). It involves simultaneous sensible heat transfer and latent heat transfer:

$$dq = dq_{sen} + dq_{lat}, \tag{4}$$

where

$$dq_{sen} = h_s dA_s (T_w - T_s), \tag{5}$$

$$dq_{lat} = h_m dA_s (W_{w,sat} - W_s) i_{fg}. \quad (6)$$

For moist air, the enthalpy is expressed as

$$i = c_{pa} T + i_{fg} W, \quad (7)$$

where c_{pa} is the specific heat of moist air, which is expressed as $c_{pa} = 1.006 + 1.86\text{W(kJ/kg} \cdot \text{K)}$.

Assuming unity Lewis factor Le_f, the convective (sensible) heat transfer coefficient on the wet side is related to the mass transfer coefficient, as follows (Lewis 1922):

$$h_m = \frac{h_s}{\text{Le}_f c_{pa}} = \frac{h_s}{c_{pa}}. \quad (8)$$

Substituting Equation 8 into Equation 6, and then substituting Equations 5 and 6 into Equation 4, gives

$$dq = \frac{h_s}{c_{pa}} dA_s (c_{pa} T_w + i_{fg} W_{w,sat} - c_{pa} T_s - i_{fg} W_s). \quad (9)$$

It is assumed that the water film temperature T_w equals the saturated water–air interface layer temperature $T_{w,sat}$, which is reasonable for a thin water film. Making this assumption, and employing Equation 7, Equation 9 can be rewritten as

$$dq = \frac{h_s}{c_{pa}} dA_s (i_{w,sat} - i_s). \quad (10)$$

It can be seen that both Equations 1 and 10 have the same functional form. If the enthalpies in Equation 10 could be expressed as a function of temperatures only (Bourdouxhe et al. 1994), Equation 10 could be used as part of a series heat transfer path with Equation 1.

In the psychometric chart, approximating the enthalpy of moist air to its wet-bulb temperature based (saturation) enthalpy will introduce some error. However, such error is relatively small over the range of temperatures considered for air conditioning. Further, the difference of those two enthaplies is linearly related, and when the enthalpy is used later, the subtraction between two states may actually offset some of this introduced error.Therefore, it is reasonable to approximate the enthalpy of moist air as a function of its wet-bulb (saturation) temperature only, namely

$$i_s = c_{pa} T_s + i_{fg} W_s \cong c_{pa} T_s^{wb} + i_{fg} W_s \left(T_s^{wb}\right). \quad (11)$$

Similarly, the enthalpy of saturated air–water interface layer can be expressed as

$$i_{w,sat} = c_{pa} T_w + i_{fg} W_{w,sat}(T_w). \quad (12)$$

It is now assumed that the enthalpy of saturated air varies linearly with wet-bulb temperature over small enough temperature ranges. In this case,

$$i = i_o + K \left(T^{wb} - T_o^{wb}\right), \quad (13)$$

where K is the "slope" of the enthalpy-saturation temperature curve, varying with the reference temperature T_o^{wb} and reference enthalpy i_o.

Substituting Equation 13 into Equation 10, and remembering that the wet-bulb temperature of the secondary air approximately equals its saturation temperature, yields

$$dq = \frac{h_s}{c_{pa}} dA_s \left(i_{w,sat} - i_s\right) \approx \frac{h_s}{c_{pa}} K dA_s \left(T_w - T_s^{wb}\right). \quad (14)$$

Equation 14 indicates that the difference between the water film temperature and the secondary-air wet-bulb temperature is the driving force for energy transfer from the water film to the secondary air stream. The term Kh_s/c_{pa} is analogous to the local heat transfer coefficient for sensible convective heat transfer, i.e., similar to h_p in Equation 2.

Based upon the above analysis, a modified effectiveness-NTU method is now applied to the thermal modeling of an IEHX. Considering the heat flux dq transferred from the primary air across the wall to the water film, and then from the water film to the secondary air (Equations 1 and 14), one obtains

$$dq = \left(\frac{1}{\frac{1}{U_{p-w} dA_p} + \frac{c_{pa}}{K h_s dA_s}}\right) \left(T_p - T_s^{wb}\right). \quad (15)$$

If dA_p equals dA_s, the overall thermal resistance $1/U$, consisting of four components and shown in Figure 2, can be presented as

$$\frac{1}{U} = \left(\frac{1}{h_p} + \frac{\delta}{k} + \frac{\delta_w}{k_w} + \frac{c_{pa}}{K h_s}\right). \quad (16)$$

For the secondary air stream, conservation of energy requires

$$dq = \dot{m}_s di_s. \quad (17)$$

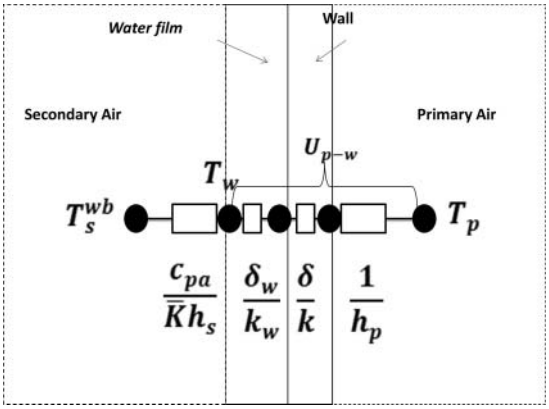

Fig. 2. Sketch of thermal resistance across the IEHX element.

Table 1. Procedure of ε -NTU method for sensible HXs and IEHXs analysis.

ε-NTU method for sensible HXs	Modified ε-NTU method for IEHXs
$C_c = \dot{m}_c c_{pc}$, $C_h = \dot{m}_h c_{ph}$	$C_c = \dot{m}_s \bar{K}$, $C_h = \dot{m}_p c_{pa}$
$C_{\min} = \min(C_c, C_h)$, $C_{\max} = \max(C_c, C_h)$, $C_r = \frac{C_{\min}}{C_{\max}}$, $NTU = \frac{UA}{C_{\min}}$	
where $\frac{1}{U} = \frac{1}{h_h} + \frac{\delta}{k} + \frac{1}{h_c}$	$\frac{1}{U} = \frac{1}{h_p} + \frac{\delta}{k} + \frac{\delta_w}{k_w} + \frac{c_{pa}}{\bar{K} h_s}$
$\varepsilon = f(NTU, C_r, \textit{flow arrangement})$	
where $\varepsilon = \frac{1-\exp(-NTU(1-C_r))}{1-C_r\exp(-NTU(1-C_r))}$ (counter flow)	
$\varepsilon = 1 - \exp[(\frac{1}{C_r})(NTU)^{0.22}\{\exp[-C_r(NTU)^{0.78}] - 1\}]$ (cross-flow, both fluids unmixed)	
$q_{\max} = C_{\min}(T_{h,i} - T_{c,i})$	$q_{\max} = C_{\min}(T_{p,i} - T^{wb}_{s,i})$
$q = \varepsilon q_{max}$	
$T_{h,o} = T_{h,i} - \frac{q}{C_h}$, $T_{c,o} = T_{c,i} + \frac{q}{C_c}$	$T_{p,o} = T_{p,i} - \frac{q}{C_h}$, $T^{wb}_{s,o} = T^{wb}_{s,i} + \frac{q}{C_c}$

Integrating Equation 17 to obtain the overall energy increment of the secondary air:

$$\dot{Q} = \dot{m}_s (i_{s,o} - i_{s,i}), \tag{18}$$

which is the derivation of the model governing differential equations. To calculate the overall heat transfer rate, Equation 17 is integrated first and then $\bar{K}$ is introduced to represent the ratio of the wet-bulb temperature difference between the wet-side inlet and outlet and their enthalpy difference; Equation 18 can then be rewritten as

$$\dot{Q} = \dot{m}_s \bar{K} \left(T^{wb}_{s,o} - T^{wb}_{s,i}\right). \tag{19}$$

Similarly, integrating Equation 3 to obtain the overall energy increment of the primary air,

$$\dot{Q} = \dot{m}_p c_{pa} \left(T_{p,i} - T_{p,o}\right). \tag{20}$$

Now, through Equations 15, 19, and 20, a modified ε-NTU method can be applied for thermal modeling of an IEHX. Table 1 summarizes the procedure for the analysis of sensible heat exchangers using the ε-NTU method and an IEHX using a modified ε-NTU method.

The main advantage of the proposed model for IEHX analysis is that the outlet conditions of the primary air and the secondary air streams, as well as the overall heat transfer rate, can be calculated using the equations in Table 1, resulting in short computational time and numerical stability for a variety of airflow arrangements (e.g., counter-flow and cross-flow).

The cooling capacity for an IEHX is determined by

$$Q_{cap} = \dot{m}_p c_{pa}(T_{p,i} - T_{p,o}). \tag{21}$$

The wet-bulb effectiveness of the IEHX based on Pescod's definition (Pescod 1979) is

$$\varepsilon^{wb} = \frac{T_{p,i} - T_{p,o}}{T_{p,i} - T^{wb}_{s,i}}. \tag{22}$$

Determination of $\bar{K}$

The value of $\bar{K}$ is needed to use the modified ε-NTU method. It can be calculated from Equations 18 and 19 by its definition:

$$\bar{K} = \frac{i_{s,o} - i_{s,i}}{T^{wb}_{s,o} - T^{wb}_{s,i}}. \tag{23}$$

However, $\bar{K}$ is not a constant, nor it is independent of wet-bulb temperature. It should also be noted that K differs from $\bar{K}$ by their definitions.

In Equation 23, both $T^{wb}_{s,o}$ and $i_{s,o}$ are unknowns. However, $i_{s,o}$ can be expressed as a function of $T^{wb}_{s,o}$ only, and such a relationship can be found by correlating saturation (wet-bulb) air temperatures and associated enthalpies from the ASHRAE Handbook (ASHRAE 2009) by means of a three-order polynomial, as shown in Figure 3. The $\bar{K}$ value may also be interpreted as the slope of the straight line connecting any two distinct points in the saturation temperature enthalpy curve, while the K is slope of the curve at a given point (Figure 3).

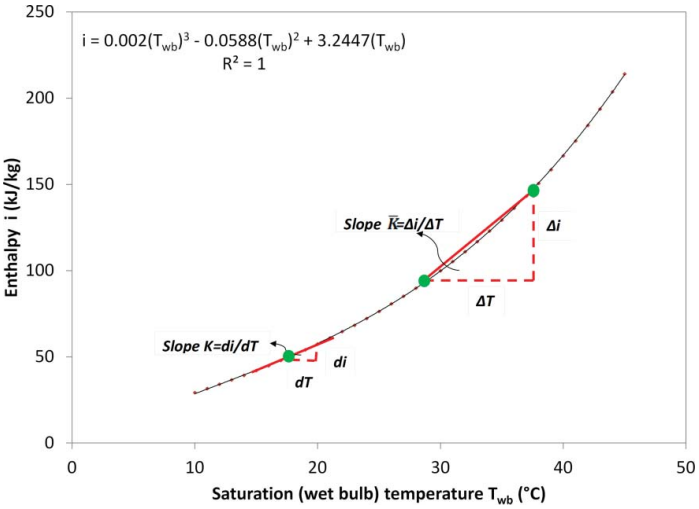

Fig. 3. Correlation of saturation air temperature versus its enthalpy and the interpretation of K and $\bar{K}$ (ASHRAE 2009) (color figure available online).

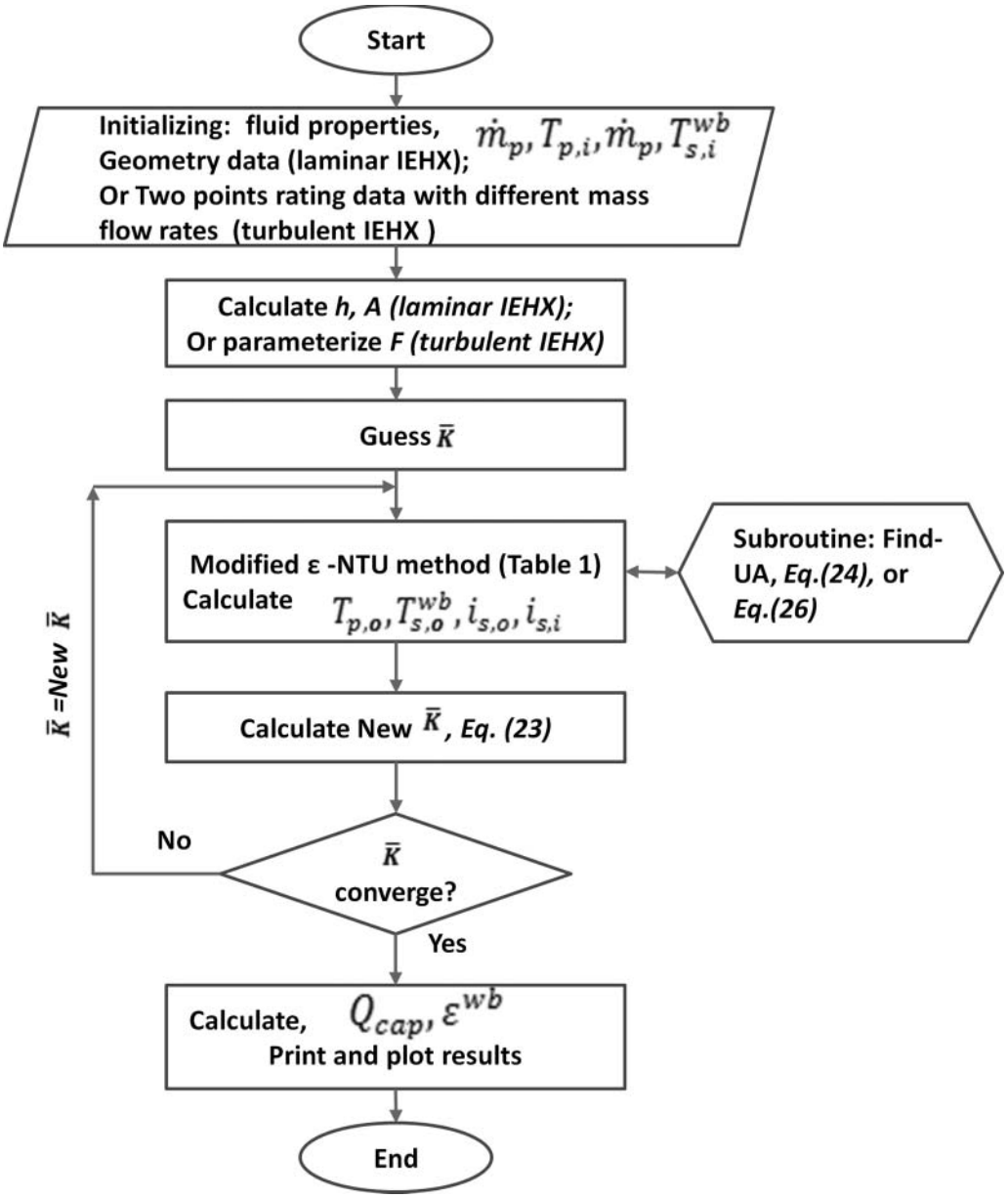

Fig. 4. Flowchart of applying the modified ε-NTU method for IEHX thermal modeling.

In Equation 23, the outlet enthalpy of the secondary air $i_{s,o}$ is a function of its outlet wet-bulb temperature $T_{s,o}^{wb}$, which is unknown before applying the modified ε-NTU method. Though one may approximate a fixed value of $\bar{K}$ using the slope at the known inlet wet-bulb temperature in Figure 3, an iterative procedure for determining the best value of $\bar{K}$ provides more accurate results. The procedure used to find the $\bar{K}$ value through iteration (Figure 4) follows.

1. Guess an intial value of $\bar{K}$ (based upon known inlet conditions).
2. Apply the modified ε-NTU method to find the value of $T_{s,o}^{wb}$.
3. Use the polynomial in Figure 3 to calculate $i_{s,o}$.
4. Calculate the new $\bar{K}$ value using Equation 23.
5. Compare the guessed $\bar{K}$ value and new $\bar{K}$ value and iterate until convergence.

It is noted that in Hasan's (2012) study, there is no discussion on how to find the value of a (similar to $\bar{K}$ in this article) or its impact on the model's accuracy. In fact, $\bar{K}$ is crucial for the accuracy of this modified ε-NTU model, which will be illustrated in the model verification section.

Determination of UA

Plate IEHX surfaces can be finned or unfinned and are operated under both dry and wet conditions. The overall thermal resistance may include the following series components:

- dry-side convection resistance,
- wall and water-film conduction resistances,

- wet-side convection resistance, and/or
- fouling effects on both the dry and wet side.

If the fouling factors are also omitted, the overall heat transfer can be expressed as an integrated version of Equation 16, and the overall UA can then be expressed as

$$\frac{1}{UA} = \frac{1}{\eta_{o,p} h_p A_p} + \frac{\delta}{k A_w} + \frac{\delta_w}{k_w A_w} + \frac{c_{pa}}{\eta_{o,s} \bar{K} h_s A_s}, \quad (24)$$

where $\eta_{o,p}$ and $\eta_{o,s}$ denote the temperature effectiveness of the dry-side total area A_p and wet-side total area A_s, respectively.

If no extended surfaces are employed on either side, both $\eta_{o,p}$ and $\eta_{o,s}$ are unity; otherwise, they are less than unity. h_p and h_s are convective heat transfer coefficients for the dry side and wet side, respectively, which are functions of surface geometries, fluid properties, and flow conditions. $\bar{K}$ is determined by the above-described iteration.

There are two common IEHX designs, namely laminar- and turbulent-flow designs. The former often uses flat surfaces arranged in narrow channels in which airflow is laminar. The latter usually utilizes extended surfaces (e.g., pin-fins) for heat transfer enhancement (at the expense of higher pressure drops), and the channel flows are partially turbulent (transit from laminar to turbulent) or fully turbulent, depending on the surface geometry and channel airflow rates.

For IEHXs with simple channel geometry and flat surfaces operated in the laminar regime, the heat transfer coefficient is constant (Kakac et al. 1987), and the overall heat transfer area is relatively easy to calculate. This is not the case for turbulent or partially turbulent flow channels with complex extended surfaces.

Determining the UA *for turbulent IEHX channel flow*

Empirical expressions for heat transfer coefficients are complex for turbulent or partially turbulent fluid flow in IEHX channels with extended surfaces (e.g., pin-fins). However, they are essentially functions of Reynolds number and surface geometry. This means that, for fixed heat transfer surfaces and air thermal properties, the heat transfer coefficients may be expressed as functions of mass flow rate only; in other words,

$$h \sim \mathrm{Re}^n \quad \text{or} \quad h \sim \dot{m}^n, \quad (25)$$

where the exponent n is found from empirical expressions for heat transfer coefficients in turbulent flow.

Coefficients F_p and F_s are introduced to address the impact of surface geometry and air thermal properties on UA calculation. Subscripts p and s donate the primary air (dry) side and the secondary air (wet) side, respectively. Though the air thermal properties may vary with channel air conditions, the impact of such variations on the heat transfer coefficients is not significant over the range of conditions typically experienced by an IEHX for air-conditioning applications. Thus, the F values are approximated as constant during the simulation. Then, if the thermal resistance of the water film and plate is negligible, Equation 24 can be rewritten as

$$\frac{1}{UA} = \frac{1}{F_p \dot{m}_p^n} + \frac{1}{F_s \bar{K} \dot{m}_s^n}. \quad (26)$$

To calculate the values of F_p and F_s in Equation 26, two points of performance rating data at different inlet mass flow rates are used to construct two independent equations and are then solved for the F values. IEHX product catalogs or performance testing data generally provide data for these two rating points. At each rating point, the $\bar{K}$ value in Equation 26 is calculated directly from Equation 23 as the inlet and outlet air conditions are known. Once the values of F are determined, the model can be used to predict the performance of an IEHX under other operating conditions. For predictions of performance under conditions other than the rating points, the $\bar{K}$ value is iteratively determined using the flowchart in Figure 4.

Determining the UA *for laminar IEHX channel flow*

Although the channel airflow is often turbulent or partially turbulent for compact IEHXs with extended surfaces, it can be laminar in some IEHXs with flat channel surfaces (Zhao et al. 2008). In this case, overall hear transfer area A can often be determined from catalog data, and the constant heat transfer coefficient h can be utilized for fully developed laminar flow in channels from the literature (Kakac et al. 1987). The temperature effectiveness $\eta_{o,p}$ and $\eta_{o,s}$ are unity for flat surfaces. Then, Equation 24 is used to find the UA values for IEHX thermal modeling, and $\bar{K}$ is determinated iteratively at each operating condition.

Figure 4 summarizes the thermal modeling procedure for IEHXs associated with the proposed modified ε-NTU method. In this procedure, the $\bar{K}$ value is obtained through iteration at every operating condition. Depending on the complexity of channel flow and surface geometries, the UA value is found from Equation 24 for simple laminar cases or from Equation 26 for complex turbulent cases

Model validation

Two data sources were used to verify the proposed model, representing the two different scenarios for UA calculation as described in the previous section. One of the scenarios is to find the UA value for an IEHX with extended pin-fin surfaces operated in a (partial) turbulent airflow regime. The second is to obtain the UA value for an IEHX with flat surfaces operated in a laminar airflow regime. The proposed modified ε-NTU method was used to simulate each scenario and then compared against the performance testing results. The methodology for finding UA was revised for each scenario to deal with those two different types of IEHX.

Model validation: turbulent heat exchanger

Peformance testing data from (Lee 2009) were used to verify the proposed thermal modeling for an IEHX with extended

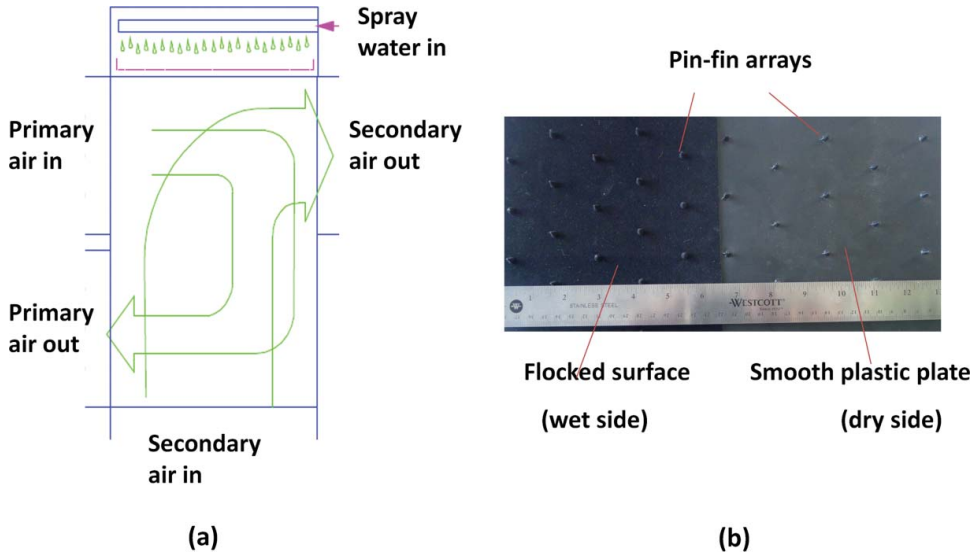

Fig. 5. (a) Schematic of turbulent-flow IEHX with C-shaped air passage in dry channel and L-shaped air passage in wet channel and (b) photos of inside surfaces of channels (color figure available online).

pin-fin surfaces operated in a turbulent or partially turbulent airflow regime. The tested IEHX has a C-shaped air passage in the dry channel and an L-shaped air passage in the wet channel (Figure 5). It is made of a thin polymer sheet (0.2 mm [0.008 in.]) with staggered pin-fins on the dry- and wet-side surfaces for heat transfer enhancement. For better water distribution, the wet-side surface is flocked. In the test, the dry-bulb temperatures and relative humidity of air entering and leaving the dry and wet channels were monitored. Also, the overall airflow rates in the dry and wet channel were measured using a nozzle box (Lee 2009).

Table 2 contains a total of 18 tests with a matrix of 9 airflow configurations and 2 different ambient inlet air conditions.

Due to geometric complexity, fluid flow and heat transfer in the C-shaped dry passage and L-shaped wet passage are too dificult to characterize practically on an a priori basis.Furthermore, both of these channels have variously shaped pins, and the heat transfer coefficient of pin-fin surfaces varies with flow rate, pin shape, and pin height-to-diameter ratio (Armstrong and Winstanley 1988). Thus, two test- points (two different flow rates) were used to determine the two F-values in Equation 26. The exponent n in Equation 26 was chosen as 0.6, based upon Pescod's experimental data (Pescod 1979). The counter-flow formula in Table 1 for effectiveness calulation was applied to this IEHX modeling. It is admitted that the flow arrangment in the tested IEHX is not a perfect counter-flow; however, the calibrated two F-values take into account such an effect. After determining the two F-values, the proposed model was used to simulate the other 16 test points.

The choice of those two rating points for the F-values determination plays a role on the accuracy of the model. However, the accuracy of the model is stable, provided that the product of those two ratios of dry-side airflow rate to wet-side flow rate for the selected two rating points exceeds 1.4.

Calculation of the conduction resistances of the wall and the water film indicates that they are negligible compared to the convective resistance terms, due to thin wall thickness (0.2 mm [0.008 in.]) and the water flow rate on the wet surface.

The comparison of model predictions with experimental data for dry-side outlet-air temperatures is presented in Figure 6. It turns out that the model predictions agree very well with the experimental data, with a maximum absolute error of 1°C (33.8°C) for all test points. The $\bar{K}$ values vary from 3132 to 4286 (J/kgK) for the 18 rating points.

Model validation: laminar heat exchanger

Experimental data from Riangvilaikul and Kumar (2010) were used to verify the proposed model for an IEHX with flat surfaces operated in a laminar flow regime. The IEHX analyzed

Table 2. Test condition matrix (Lee 2009).

		Inlet dry-/wet-bulb air temperature, °F (°C)	Flow rate, CFM (m^3/h)
Western maximum	Wet side	80/67 (26.7/19.4)	Matrix of all combinations of (500, 1000, 1500) × (500, 1000, 1500) ([850, 1700, 2550] × [850, 1700, 2550])
	Dry side	105/70 (40.6/21.1)	
Western summer	Wet side	76/64 (24.4/17.8)	Matrix of all combinations of (500, 1000,1500) × (500, 1000,1500) ([850, 1700, 2550] × [850, 1700, 2550])
	Dry side	95/66 (35/18.9)	

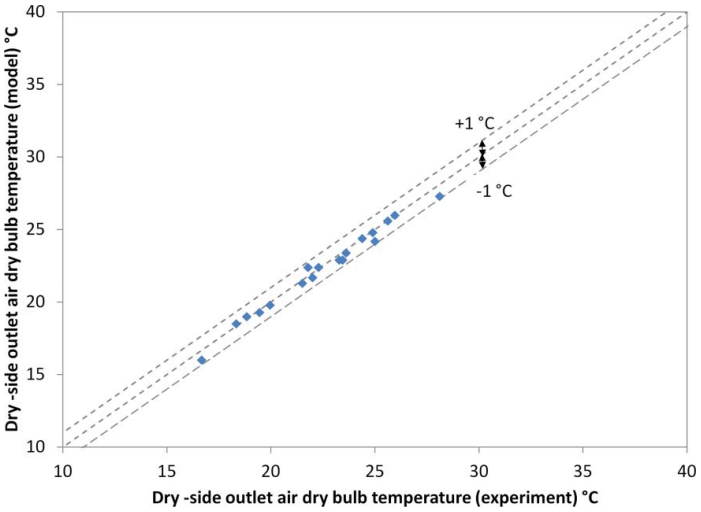

Fig. 6. Comparison of model predictions for dry-side outlet-air dry-bulb temperatures with experimental data (color figure available online).

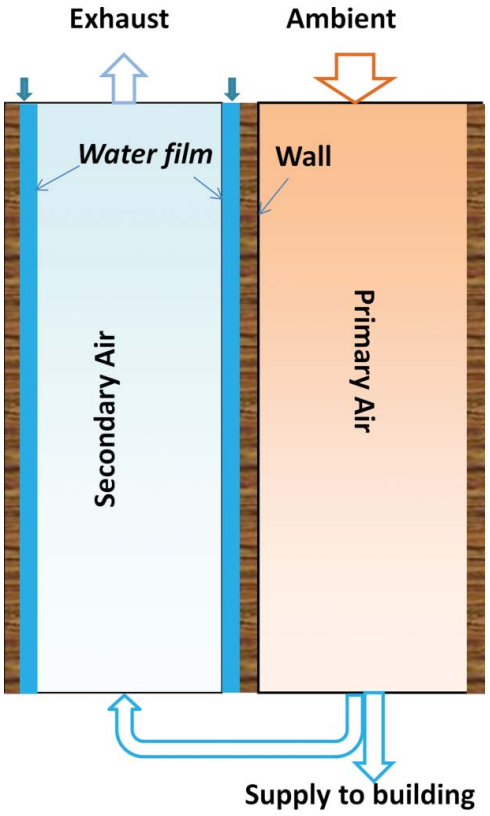

Fig. 7. Schematic of regenerative-type IEHX used for model verification (Riangvilaikul and Kumar 2010) (color figure available online).

is a regenerative-type heat exchanger with a counter-flow arrangement (Figure 7). The inlet air goes through the dry channel, and its outlet flow is split into two air streams: one is the supply air to the conditioned space and the other goes through the wet channel and exhausts to ambient. A detailed description of the heat exchanger, test facility, and measurement processcan be found in Riangvilaikul and Kumar (2010). The tested IEHX wall material is a thin-sheet polymer with an evenly coated cotton sheet on the wet-side surface. Both the dry and wet (rectangular) channels are 80 mm (3.15 in.) in width, 1200 mm (47.24 in.) in length, and 5 mm (0.197 in.) in channel gap. Thus the heat transfer area on the dry and wet side can be calculated in a straightforward manner. The dry-bulb and wet-bulb temperatures of air entering and leaving the dry and wet channels were measured. In addition, the air velocities in the dry and wet channels were monitored. For all tests, the fraction of air diverted from the dry channel to the wet channel was kept at 0.33.

Two groups of tests were conducted to investigate the dry-side outlet air temperature at varying inlet air conditions and different channel air velocities.

- Test A: A matrix of five temperatures (25, 30, 35, 40, and 45°C [77, 86, 95, 104, and 113°F]) and four humidity ratio levels (0.0069, 0.0112, 0.020, and 0.0264) were used as inlet air conditions at a dry-channel air velocity of 2.4 m/s (7.9 fps). The corresponding outlet air temperatures were measured.
- Test B: A matrix of six dry-channel air velocities (1.5, 2.4, 3.3, 4.2, 5.1, and 6.0 m/s [4.9, 7.9, 10.8, 13.8, 16.7, and 19.7 fps]) and two levels of humidity ratio (0.0112 and 0.019) were tested at a constant inlet air temperature of 34°C (93°F). The corresponding outlet air temperatures were measured.

A calculation of the Reynolds numbers for the airflows in both and dry and wet channels for all test points indicates that channel flows are laminar. Also, the entry effect was assumed negligible, as the ratio of channel length to channel gap size is 240. Thus, a constant convective heat transfer coefficient was used (Incropera 1996). The channel geometry as well as the heat transfer coefficients were used to calculate the *UA* value.

The results of comparing model predictions with experimental data from Test A and Test B are presented in Figures 8 and 9, respectively, for the dry-side outlet air temperatures at different intake air conditions (Figure 8) and different intake channel air velocities (Figure 9). The $\bar{K}$ values vary from 3575 to 6017 J/kg.k for the 29 rating points.

Figure 8 compares the model predictions with experimental data for dry-side outlet air temperature at different inlet ambient air conditions (matrix of five temperatures and four humidities), while the inlet dry-side air velocity is fixed at 2.4 m/s (7.9 fps), which covers dry, intermediate, and humid ambient air conditions. Figure 9 compares the model predictions with experimental data for the dry-side outlet air temperature at six different inlet air velocities. As shown in Figures 8 and 9, the model predictions agree well with the experimental data,with a maximum absolute error of 2°C (35.6°F) for all testing points. A careful examination of Figures 8 and 9 indicates that the model tends to under-predict the outlet air temperatures and that the discrepancy decreases from about 2°C to 0.3°C (35.6°F to 32.5°F) as the humidity ratio increases from 0.069 to 0.0264 (Figure 8). A possible reason for this discrepancy is discussed in what follows. The hypothesis is that

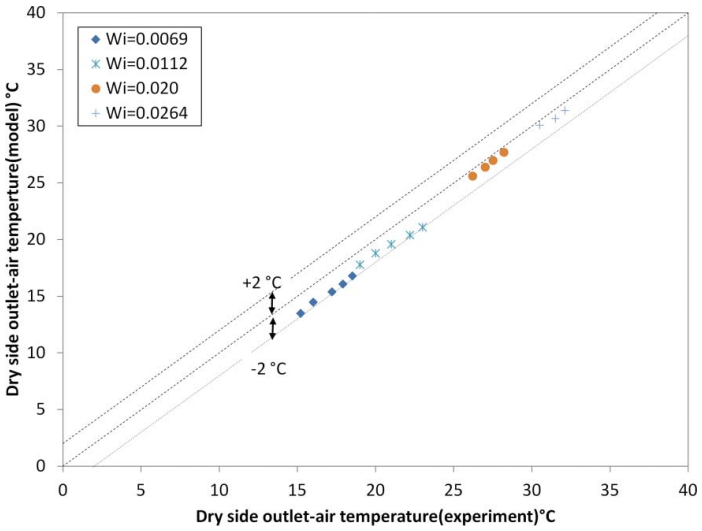

Fig. 8. Comparison of model predictions for dry-side outlet-air temperature with experimental data at five different dry-side inlet-air temperatures and four different dry-side inlet-air humidity ratio (color figure available online).

the assumption of a unity Lewis factor might be invalid for water evaporation into a very cold and dry (low humidity ratio) air stream.

Discussion

A possible reason for the discrepancy between model predictions and experimental data for laminar flow heat exchanger (Figures 8 and 9) is that the unity Lewis factor assumption may be invalid to describe water evaporation into a very cold and dry air stream.

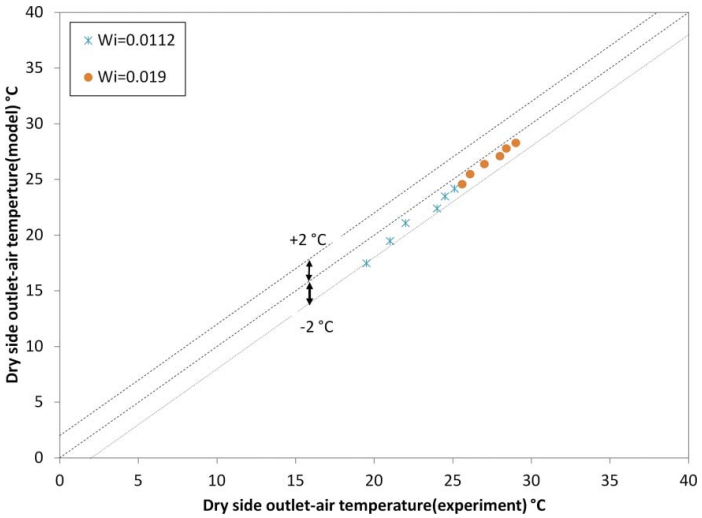

Fig. 9. Comparison of model predictions for dry-side outlet-air temperature with experimental data for dry-side air operated at a combination of six different air velocities and two levels of humidity ratio (color figure available online).

The Lewis factor, or Lewis relation (Lewis 1922), is an indication of the relative rates of heat and mass transfer in an evaporative process. Lewis (1933) stated that the Lewis factor should be approximately unity for air/water mixtures. This unity Lewis factor approximation has been widely adopted for water evaporation modeling in HVAC practice, such as for cooling towers (Merkel 1925) and wet surface heat exchangers (Erens and Dreyer 1993). However, this unity Lewis factor approximation was criticized by Bourillot (1983), who introduced a correction (approximately 0.92) to account for the impact of inlet air humidity ratio on cooling tower performance prediction. Häszler (1999) also doubted the unity Lewis factor assumption and stated that the Lewis factor ranges from 0.5 to 1.3. He also stated that the unity Lewis factor approximation is not valid when the humidity potential is large. Kloppers and Kroger (2005b) utilized a verified model to analyze the influence of different Lewis factors ($Le_f = 0.5$, 0.92, and 1.3) on cooling tower performance prediction. Their results indicate the impact of Lewis factor variation on wet cooling tower performance prediction diminishes when the entering ambient air is relatively hot and humid. However, they also indicated that the Lewis factor impact can be quite significant when the entering ambient air is very cold and dry.

The water evaporation process in the wet channel of an IEHX is quite similar to that in a indirect-contact cooling tower. According to the simulation results in Figure 8, it is hypothesized that the colder and drier the air on the wet side, the more significant the impact of Lewis-factor variation is on the proposed IEHX thermal modeling. To investigate this hypothesis, the proposed model was used to predict the performance of the above regenerative IEHX at three Lewis factors, namely $Le_f = 0.5$, 1.0, and 1.3, for a variety of wet-side inlet air conditions. Figure 10 presents the results, indicating that the impact of Lewis factor variation on this regerative IEHX performance prediction can be quite significant (8% between Lewis factors of 0.5 and 1.3) when the wet-side entering air is cold and dry (temperature = 15°C [59°F], humidity ratio =

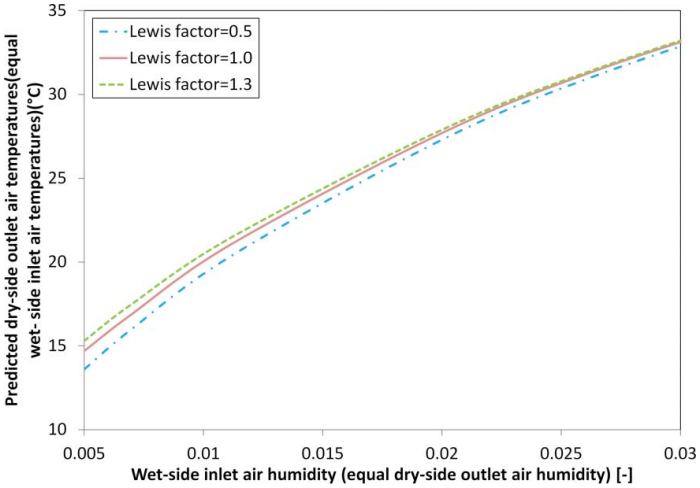

Fig. 10. Variation of the predicted dry-side outlet-air temperatures of regenerative IEHX at different wet-side inlet air humidities for three different Lewis factors (color figure available online).

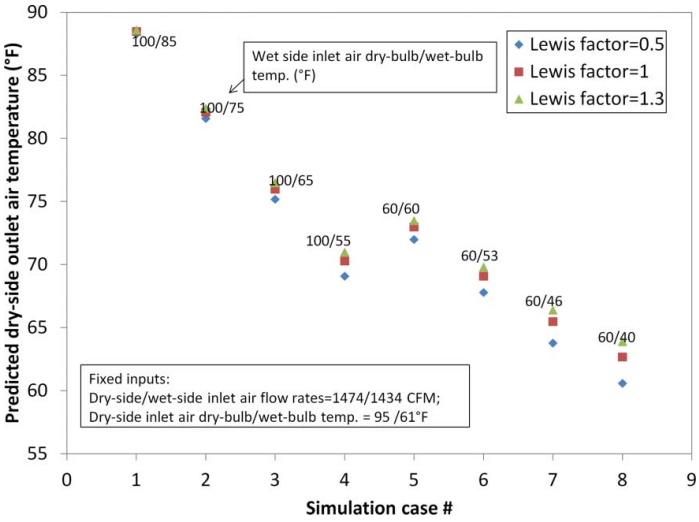

Fig. 11. Variation of the predicted dry-side outlet-air temperatures of turbulent IEHX at different wet-side inlet air conditions for three different Lewis factors (color figure available online).

0.005). Figure 10 also indicates that the impact of Lewis factor diminishes dramatically (1%) when the wet-side entering air is relatively hot and humid (temperature = 31°C [88°F], humidity ratio = 0.0264). This result agrees with Kloppers and Kroger's (2005b) analysis.

To further examine the hypothesis that colder, drier wet-side inlet air introduces discrepancies in IEHX simulation results due to the assumed Lewis factor, a number of simulations were conducted using the proposed model for turbulent IEHXs. A 2×4 matrix for wet-side inlet air conditions ranging from hot/humid to cold/dry was chosen as an inlet variable. The predicted dry-side outlet air temperatures based on three different Lewis factors ($Le_f = 0.5$, 1.0, and 1.3) for each simulation were compared, and the results are shown in Figure 11, which again confirms the hypothesis that colder, drier wet-side inlet air introduce a larger sensitivity to Lewis factors.

This above analysis suggests that if a unity Lewis factor is assumed, the discrepancy of model predictions with experimental data can be significant when the wet-side inlet air is relatively cold and dry. Further investigation is needed to find a proper Lewis factor for the thermal modeling of an IEHX in such a situation.

Conclusion

This article proposes a methodology for thermal modeling of IEHXs at varying inlet air conditions and different airflow rates, designed for system-level hybrid IEC/DX energy simulation. The proposed model is analogous to the ε-NTU method for sensible heat exchangers, introducing an iteratively determined $\bar{K}$ for the wet side of the heat exchanger. Two different ways for determining the overall UA for the exchanger are demonstrated. Existing experimental data from two distinct IEHXs were used to verify the proposed modeling methodology. The model predictions are in good agreement with this experimental data from the literature. An examination of the Lewis factor impact on evaporation processes using this model indicates that the approximation of unity for the Lewis factor may not be valid when the inlet air to the wet side is relatively cold and dry.

Nomenclature

A = heat transfer area
C = fluid capacity
c_{pa} = specific heat of moist air
d = half air passage height
F = coefficient to be calibrated in UA calculation
h = convective heat transfer coefficient
h_m = mass transfer coefficient
i = enthalpy
i_{fg} = heat of vaporization for water at 0°C (32°F)
k = thermal conductivity
K = slope of enthalpy versus saturation temperature curve
$\bar{K}$ = ratio of enthalpy change versus wet-bulb temperature change in wet side of IEHX
Le_f = Lewis factor
$\dot{m}$ = mass flow rate of fluids
NTU = number of heat transfer units
q = heat transfer rate
$\dot{Q}$ = overall heat transfer rate
Q_{cap} = cooling capacity
Re = Reynolds number
T = dry-bulb temperature
U = overall heat transfer coefficient
W = humidity ratio of air stream

Greek symbols

δ = thickness of plate wall/water film
ε = effectiveness
η = temperature effectiveness
ρ = density of air

Subscripts

c = cold fluid
h = hot fluid
i = inlet
o = outlet
p = primary air
s = secondary air
sat = saturated
sen = sensible
w = water film

Superscripts

n = exponent coefficient
wb = wet-bulb temperature

Acknowledgments

The authors would like to acknowledge support from the California Energy Commission that funded this work (grant 500-08-042). They also thank Eric Lee (Halperis Energy) for providing test data on the turbulent IEHX for the model verification.

References

Armstrong, J., and D. Winstanley. 1988. A review of staggered array pin fin heat-transfer for turbine cooling applications. *Journal of Turbomachinery—Transactions of the ASME* 110(1):94–103.

ASHRAE. 2009. *ASHRAE Handbook Fundamentals*. Atlanta, GA, American Society of Heating, Refrigerating and Air-Conditioning Engineers, Inc.

Bourdouxhe, P., M. Grodent, and J. Lebrun. 1994. Cooling-tower model developed in a toolkit for primary HVAC system energy calculation—Part 1: Model description and validation using catalog data. *Proceedings of the Fourth International Conference on System Simulation in Buildings, Liège, Belgium*.

Bourillot, C. 1983. On the hypothesis of calculating the water flowrate evaporated in a wet cooling tower. EPRI Report CS-3144-SR. Palo Alto, CA: Electric Power Research.

Braun, J.E., S.A. Klein, and J.W. Mitchell. 1989. Effectiveness models for cooling towers and cooling coils. *ASHRAE Transactions Research* 95:167–74.

Elberling, L. 2006. Laboratory evaluation of the Coolerado cooler indirect evaporative cooling unit. San Ramon, CA: Pacific Gas and Electric Company.

ElDessouky, H.T.A., A. AlHaddad, and F. AlJuwayhel. 1997. A modified analysis of counter flow wet cooling towers. *Journal of Heat Transfer—Transactions of the ASME* 119(3):617–26.

EnergyPlus simulation software. http://apps1.eere.energy.gov/buildings/energyplus/.

Erens, P.J., and A.A. Dreyer. 1993. Modeling of indirect evaporative air coolers. *International Journal of Heat and Mass Transfer* 36(1):17–26.

Gandhidasan, P. 2004. A simplified model for air dehumidification with liquid desiccant. *Solar Energy* 76(4):409–16.

Hasan, A. 2012. Going below the wet-bulb temperature by indirect evaporative cooling: Analysis using a modified epsilon-NTU method. *Applied Energy* 891:237–45.

Häszler, R. 1999. Einflusz von Kondensation in der Grenzschicht auf die Wärme- und Stoffübertragung an einem Rieselfilm. *Fortschritt-Berichte VDI* 3:615.

Hsu, S.T., Z. Lavan, and W.M. Worek. 1989. Optimization of wet-surface heat-exchangers. *Energy* 14(11):757–70.

Incropera, F.P. 1996. *Fundamentals of Heat and Mass Transfer*. New York, John Wiley & Sons.

Kakac, S., R.K. Shah, and W. Aung. 1987. *Handbook of Single Phase Convective Heat Transfer*. New York., Wiley.

Kays, W.M. 1984. *Compact Heat Exchangers*. New York, McGraw-Hill.

Kloppers, J.C., and D.G. Kroger. 2005a. A critical investigation into the heat and mass transfer analysis of counterflow wet-cooling towers. *International Journal of Heat and Mass Transfer* 48(3–4):765–77.

Kloppers, J.C., and D.G. Kroger. 2005b. The Lewis factor and its influence on the performance prediction of wet-cooling towers. *International Journal of Thermal Sciences* 44(9):879–84.

Lee, E. 2009. Indirect evaporative heat recovery ventilator heat exchanger (final report). from http://wcec.ucdavis.edu/wp-content/uploads/2012/10/IEHRV-BERG-Final-Report.pdf.

Lewis, W.K. 1922. The evaporation of a liquid into a gas. *Transactions of the ASME* 44:325–40.

Lewis, W.K. 1933. The evaporation of a liquid into a gas—a correction. *Mechanical Engineering* 55:567–73.

Maheshwari, G.P., F. Al-Ragom, and R.K. Suri. 2001. Energy-saving potential of an indirect evaporative cooler. *Applied Energy* 69(1):69–76.

Merkel, F. 1925. Verdunstungskühlung. *VDI-Zeitchrift* 70:123–8.

Pescod, D. 1979. A heat exchanger for energy saving in an air-conditioning plant. *ASHRAE Transactions Research* 85(Part 2):238–51.

Poppe, M., and H. Rögener. 1984. Evaporative cooling systems. *VDI-Wärmcatlas*.

Riangvilaikul, B., and S. Kumar. 2010. An experimental study of a novel dew point evaporative cooling system. *Energy and Buildings* 42(5):637–44.

Stabat, P., and D. Marchio. 2004. Simplified model for indirect-contact evaporative cooling tower behaviour. *Applied Energy* 78(4):433–451.

Zhao, X., J.M. Li, and S.B. Riffat. 2008. Numerical study of a novel counter-flow heat and mass exchanger for dew point evaporative cooling. *Applied Thermal Engineering* 28(14–15):1942–1951.